J|A|C|S ARTICLES

Published on Web 07/27/2010

# Theoretical Study of Substituted PBPB Dimers: Structural Analysis, Tetraradical Character, and Excited States

Franziska Bell,[†] David Casanova,*[,‡] and Martin Head-Gordon[†]

*Department of Chemistry, University of California, and Chemical Sciences Division, Lawrence Berkeley National Laboratory, Berkeley, California 94720, and Institut de Química Teòrica i Computacional (IQTCUB), Universitat de Barcelona, Martí i Franquès 1-11, 08028 Barcelona, Spain*

Received June 1, 2010; E-mail: davidcasanovacasas@ub.edu

***Abstract:*** The radicaloid nature of *para* and *meta* 1,3-diborata-2,4-diphosphoniocyclobutane-1,3-diyl doubly substituted benzene is assessed from several electronic structure perspectives. Orbital occupation numbers computed by perfect pairing (PP), complete active space SCF (CASSCF), and restricted active space double spin-flip (RAS-2SF) reveal the presence of less than one unpaired electron in the planar molecules. Thus, the surprising stability of the "*para* tetraradical" can be rationalized by its moderate extent of radical character. Estimation of the delocalization energy, low-lying excited states, and short and long-range magnetic coupling constants all indicate a rather weak interaction to occur between two singlet PBPB units. Communication between two triplet units was found to be negligible. Comparison between *para* and *meta* isomers confirms a distinctly larger communication *via* the $\pi$ framework for the former. However, this communication, which was recently proposed to be the main factor for the different behavior of *meta* and *para* isomers regarding their preferred geometries, was found to account for only one-third of their energy difference. The study shows the important contribution of steric and/or electronic effects of the bulky $^{i}$Pr and $^{t}$Bu substituents on P and B.

## Introduction

In the search for molecular materials with new interesting properties, main group element radicaloid systems have become an intensively studied topic in the past and recent years.[1−4] Among them, diradicals are molecules featuring two unpaired electrons, each of which is occupying two degenerate or nearly degenerate molecular orbitals (MOs).[5−8] Due to the unpaired nature of these systems, diradicals are usually very reactive[8,9] and thus short-lived. The linkage of two or more radical moieties appears to be one of the most successful and extensively studied strategies to yield molecules of polyradicaloid character. Moreover, this procedure allows the achievement of different electronic properties by modifying the nature of the linker practically at will.[10,11]

Particularly interesting is the catenation of singlet diradical monomers, which is predicted to yield antiferromagnetic low-spin polymers.[12,13] Their half-filled electron bands would confer the capability for metallic conduction without doping.[9,14−17] In this direction, several carbon based di-[18] and tetraradical[10,19−25] prototypes have been prepared, but their extremely short half-life constitutes a major drawback. However, recently, a few stable diradicals based on main-group elements have been isolated.[26−35] Among them, 1,3-diborata-2,4-diphosphoniocyclobutane-1,3-diyls (**1A** in Figure 1) yield a "localized singlet diradical that is indefinitely stable at room temperature" upon

[†] University of California and Lawrence Berkeley National Laboratory.
[‡] Universitat de Barcelona.

(1) Smith, M. B.; March, J. *March's Advanced Organic Chemistry; Reactions, Mechanisms and Structure*; Wiley Interscience: New York, 2001.
(2) Power, P. P. *Chem. Rev.* **2003**, *103*, 789–810.
(3) Grützmacher, H.; Breher, F. *Angew. Chem., Int. Ed.* **2002**, *41*, 4006–4011.
(4) Forrester, A. R.; Hay, J. M.; Thomson, R. H. *Organic Chemistry of Stable Free Radicals*; Academic Press: London, 1968.
(5) Berson, J. A. *Science* **1994**, *266*, 1338–1339.
(6) Borden, W. T. *Encyclopedia of Computational Chemistry*; Wiley-Interscience: New York, 1998.
(7) Borden, W. T.; Iwamura, H.; Berson, J. A. *Acc. Chem. Res.* **1994**, *27*, 109–116.
(8) Pedersen, S.; Herek, J. L.; Zewail, A. H. *Science* **1994**, *266*, 1359–1364.
(9) Zewail, A. H. *Angew. Chem., Int. Ed.* **2000**, *39*, 2586–2631.
(10) Rajca, A. *Chem. Rev.* **1994**, *94*, 871–893.
(11) Rovira, C.; Ruiz-Molina, D.; Elsner, O.; Vidal-Gancedo, J.; Bonvoisin, J.; Launay, J.-P.; Veciana, J. *Chem.—Eur. J.* **2001**, *7*, 240–250.
(12) Berson, J. A. *Acc. Chem. Res.* **1997**, *30*, 238–244.
(13) *Conjugated polymers and Related Materials*; Salaneck, W. R., Lundström, I., Råånby, B., Eds.; Oxford: New York, 1993.
(14) *Conjugated Polymers and Related Materials*; Oxford University Press: Oxford, 1991.
(15) Albright, T. A.; Burdett, J. K.; Whangbo, M.-H. *Orbital Interactions in Chemistry*; Wiley-Interscience: New York, 1985.
(16) Bumm, L. A.; Arnold, J. J.; Cygan, M. T.; Dunbar, T. D.; Burgin, T. P.; Jones II, L.; Allara, D. L.; Tour, J. M.; Weiss, P. S. *Science* **1996**, *271*, 1705–1707.
(17) Whangbo, M.-H. In *Extended Linear Chain Compounds*; Miller, J. S., Ed.; Plenum: New York, 1982; Vol. II.
(18) Adam, W.; Borden, W. T.; Burda, C.; Foster, H.; Heidenfelder, T.; Heubes, M.; Hrovat, D. A.; Kita, F.; Lewis, S. B.; Scheutzow, D.; Wirz, J. *J. Am. Chem. Soc.* **1998**, *120*, 593–594.
(19) Crayston, J. A.; Devine, J. N.; Walton, J. C. *Tetrahedron* **2000**, *56*, 7829–7857.
(20) Dougherty, D. A. *Acc. Chem. Res.* **1991**, *24*, 88–94.
(21) Koga, N.; Karasawa, S. *Bull. Chem. Soc. Jpn.* **2005**, *78*, 1384–1400.
(22) Lu, H. S. M.; Berson, J. A. *J. Am. Chem. Soc.* **1996**, *118*, 265–266.
(23) Lu, H. S. M.; Berson, J. A. *J. Am. Chem. Soc.* **1997**, *119*, 1428–1438.
(24) Miller, J. S.; Epstein, A. J. *MRS Bull.* **2000**, *25*, 21.
(25) Rajca, A. *Adv. Phys. Org. Chem.* **2005**, *40*, 153.

 **10.1021/ja104772w** 

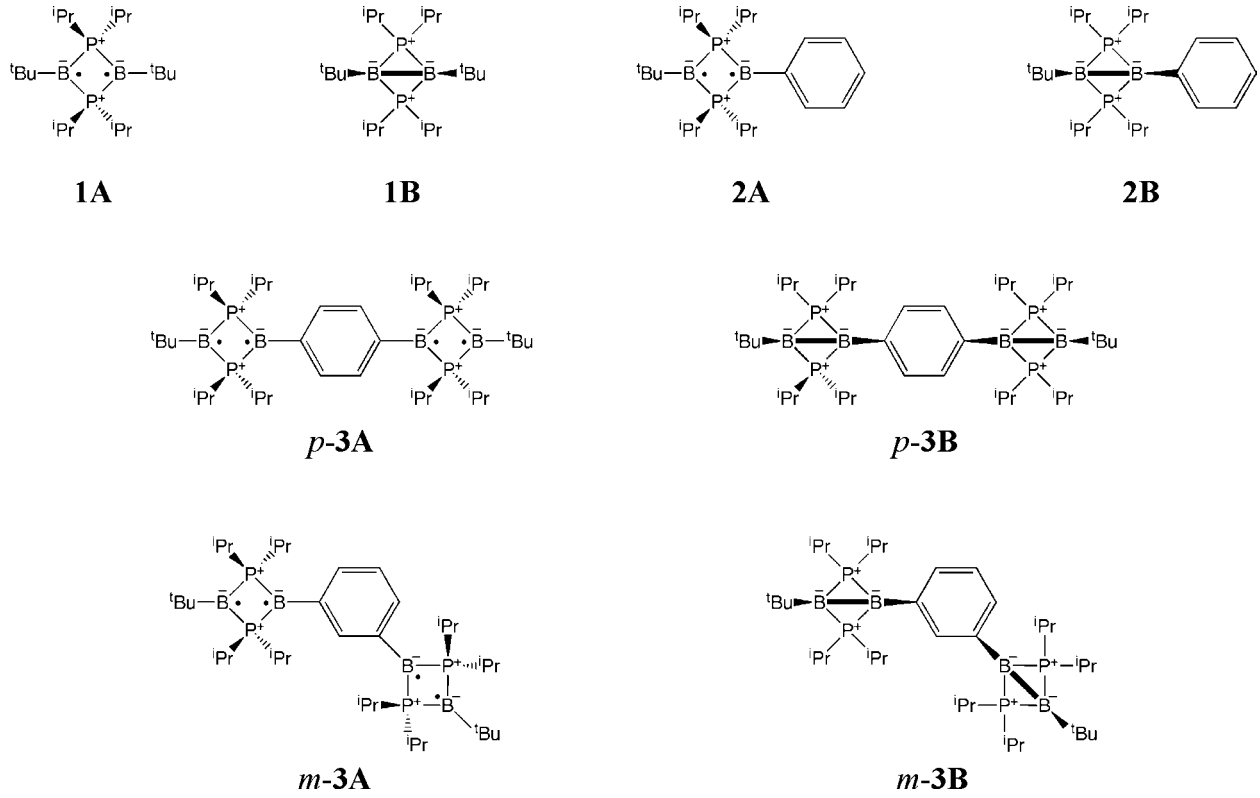


***Figure 1.*** Overview of the most important structures. Para and meta conformations are specified by *p*- and *m*- prefixes. **A** and **B** labeling indicates planar (1,3-diborata-2,4-diphosphoniocyclobutane-1,3-diyl) and bicycle (1,3-diborata-2,4-diphosphoniobicyclo[1.1.0]butane) rearrangements of the PBPB moieties, respectively. Numbers **1**, **2**, and **3** correspond to PBPB monomer, phenyl-PBPB molecule, and PBPB dimer, respectively.

adequate choice of substituents.[36] Thus these systems are one of the currently most promising building blocks for low-spin polymers. This made them subject to several experimental[37,38] as well as theoretical studies.[39−43]

Recently, Rodriguez et al. catenated two of these moieties successfully *via para*- and *meta*-phenylene linkers.[44] Experimental data in the solid state as well as in solution of these new compounds indicate that the topology of the linker plays a crucial role in their structural and electronic properties. X-ray diffraction analysis reveals that the *para* isomer exhibits virtually planar PBPB moieties, which are coplanar to the phenyl ring (*p*-**3A** in Figure 1), and was proposed to be the first stable singlet tetraradical.[44] On the other hand, the *meta*-phenylene linker favors a bis(bicycle) arrangement (*m*-**3B** in Figure 1) and the system does not feature any radicaloid character. The authors ascribed the stability of *p*-**3A** to a weak "communication" *via* the $\pi$ framework between the two diradical sites and, therefore, as the cause for the marked conformational differences between the two isomers.[45]

In solution, the *para* planar structure *p*-**3A** is in equilibrium with the bis(bicyclic) analogue *p*-**3B** (Figure 1) indicating a small energy difference between these two bond stretch isomers. This equilibrium is displaced to *p*-**3A** at low temperatures and to the bis(bicyclic) form at high temperatures. On the other hand, no such equilibrium was found for the *meta* conformation. The only structure observed was the bis(bicyclic) form *m*-**3B**.[46]

The absence of EPR signal in both solution and the solid state indicates that *p*-**3A** features a singlet ground state, but the absence of an EPR signal is not definitive. Hence, the ground state multiplicity of the systems needs to be confirmed.

(26) Cox, H.; Hitchcock, P. B.; Lappert, M. F.; Pierssens, L. J.-M. *Angew. Chem., Int. Ed.* **2004**, *43*, 4500–4504.
(27) Cui, C.; Brynda, M.; Olmstead, M. M.; Power, P. P. *J. Am. Chem. Soc.* **2004**, *126*, 6510–6511.
(28) Niecke, E.; Fuchs, A.; Nieger, M. *Angew. Chem., Int. Ed.* **1999**, *38*, 3028–3031.
(29) Ito, S.; Kikuchi, M.; Sugiyama, H.; Yoshifuji, M. *J. Organomet. Chem.* **2007**, *692*, 2761–2767.
(30) Sebastian, M.; Hoskin, A.; Nieger, M.; Nyulászi, L.; Niecke, E. *Angew. Chem., Int. Ed.* **2005**, *44*, 1405–1408.
(31) Sebastian, M.; Nieger, M.; Szieberth, D.; Nyulászi, L.; Niecke, E. *Angew. Chem., Int. Ed.* **2004**, *43*, 637–641.
(32) Sugiyama, H.; Ito, S.; Yoshifuji, M. *Angew. Chem., Int. Ed.* **2003**, *42*, 3802–3804.
(33) Yoshifuji, M.; Arduengo, A. J., III; Konovalova, T. A.; Kispert, L. D.; Kikuchi, M.; Ito, S. *Chem. Lett.* **2006**, *35*, 1136–1137.
(34) Abe, M.; Adam, W.; Heidenfelder, T.; Nau, W. M.; Zhang, X. *J. Am. Chem. Soc.* **2000**, *122*, 2019–2026.
(35) Abe, M.; Kubo, E.; Nozaki, K.; Matsuo, T.; Hayashi, T. *Angew. Chem., Int. Ed.* **2006**, *45*, 7828–7831.
(36) Scheschkewitz, D.; Amii, H.; Gornitzka, H.; Schoeller, W. W.; Bourissou, D.; Bertrand, G. *Science* **2002**, *295*, 1880–1881.
(37) Amii, H.; Vranicar, L.; Gornitzka, H.; Bourissou, D.; Bertrand, G. *J. Am. Chem. Soc.* **2004**, *126*, 1344–1345.
(38) Rodriguez, A.; Olsen, R. A.; Ghaderi, N.; Scheschkewitz, D.; Tham, F. S.; Mueller, L. J.; Bertrand, G. *Angew. Chem., Int. Ed.* **2004**, *43*, 4880–4883.
(39) Cheng, M.-J.; Hu, C.-H. *Mol. Phys.* **2003**, *101*, 1319–1323.
(40) Jung, Y.; Head-Gordon, M. *ChemPhysChem* **2003**, *4*, 522–525.
(41) Jung, Y.; Head-Gordon, M. *J. Phys. Chem. A* **2003**, *107*, 7475–7481.
(42) Schoeller, W. W.; Rozhenko, A.; Bourissou, D.; Bertrand, G. *Chem.—Eur. J.* **2003**, *9*, 3611–3617.
(43) Seierstad, M.; Kinsinger, C. R.; Cramer, C. J. *Angew. Chem., Int. Ed.* **2002**, *41*, 3894–3896.
(44) Rodriguez, A.; Tham, F. S.; Schoeller, W. W.; Bertrand, G. *Angew. Chem., Int. Ed.* **2004**, *43*, 4876–4880.
(45) Soleilhavoup, M.; Bertrand, G. *Bull. Chem. Soc. Jpn.* **2007**, *80*, 1241–1252.
(46) Rodriguez, A.; Fuks, G.; Bourg, J.-B.; Bourissou, D.; Tham, F. S.; Bertrand, G. *Dalton Trans.* **2008**, 4482–4487.

Moreover, although *p*-**3A** was predicted to exhibit tetradicaloid character, its extent has not yet been quantified. The radical character concept is mainly based on chemical intuition, as there is no quantum mechanical operator that defines the extent of pairing unambiguously. Consequently, there can be no direct measurement of radical character.

Although experimental efforts and preliminary computational analysis have provided a better understanding of these systems, several questions still remain open for a full comprehension: Can calculations confirm the presence of a $\pi$ interaction between the two PBPB units in the *para* compound *p*-**3A**? Is this interaction the sole reason for the geometrical differences observed between *meta* and *para* isomers? Is the electronic ground state of *p*-**3A** a singlet? What is the extent of its tetraradical character?

This work comes to answer these and other related questions for the *para*-phenylene and *meta*-phenylene linkage of two PBPB skeletons. The present study is organized as follows: first, we detail the computational tools employed. Then, we discuss the main structural characteristics, the stability of the different species, and the tetraradical nature and magnetic couplings of planar systems. Finally, the main conclusions will be outlined.

## Computational Details

Molecular geometry optimizations and frequency analysis were performed at the B3LYP level in combination with the 6-31G(d) basis set.[47] The adequacy of the 6-31G(d) basis set was tested against the much larger 6-311G(3df,2pd) basis[48,49] set for the H-substituted molecular models (see below), and hardly any effect on the optimized geometries was observed. The 6-31G(d) basis set was also employed in all other electronic structure computations. Relative energy stability between bond strech and *meta*/*para* isomers was explored by B3LYP and the resolution-of-identity (RI)[50−53] implementation[54,55] of the coupled-cluster (CC) formulation of perfect pairing (PP).[56,57] The VDZ auxiliary basis[58] for RI-MP2 was chosen in the RI approach. The tetraradicaloid character of planar molecules was determined through the orbital occupation numbers from the one particle density matrix of PP, complete active space SCF (CASSCF)[59] with four orbitals and four electrons in the active space, and the restricted active space double spin-flip (RAS-2SF) method,[60] and by means of the perfect quadruples (PQ),[61] CASSCF(4,4), and RAS-2SF single amplitudes of the $\hat{T}_4$ cluster operator. All RAS-2SF calculations were performed within the (*hole*, *particle*) truncation and using a restricted open shell (ROHF) high spin quintet as reference to obtain $M_S = 0$ states. In order to understand the role of the substituent groups in phosphorus and boron atoms, and for the sake of lower computational cost as well, calculations were also carried out on model systems, in which hydrogen atoms replace the $^t$Bu and $^i$Pr groups. These molecules will be labeled analogously to their parent compounds (see Figure 1), but with an **H** at the end. Since all H-substituted model systems feature the bis(bicyclic) geometry as their ground state, optimizations of the planar conformations were carried out by restricting the geometry optimization to the corresponding symmetry point group.

Most of the calculations were performed using a development version of the Q-CHEM package.[62] Complete active space SCF was carried out with the 2009 version of GAMESS.[63]

***Table 1.*** Experimental and B3LYP/6-31G(d) Optimized Most Relevant Atomic Distances (in Å) and the BPPB Dihedral Angle ($\delta$ in deg) of Planar Singlet Structures (**A**)[a]

| | | | | | experimental | |
|---|---|---|---|---|---|---|
| planar structures | **1A** | **2A** | *p*-**3A** | *m*-**3A** | **1A**[36,37] | *p*-**3A**[44] |
| B1···B2 | 2.59 (2.56) | 2.59 (2.59) | 2.59 (2.58) | 2.59 (2.58) | 2.559 | 2.568 |
| P···P | 2.80 (2.78) | 2.80 (2.77) | 2.80 (2.77) | 2.80 (2.78) | 2.787 | 2.792 |
| B1−$C_{tBu}$ | 1.61 | 1.61 | 1.61 | 1.61 | 1.597 | 1.598 |
| B2−$C_{Ph}$ | − | 1.55 (1.53) | 1.54 (1.53) | 1.56 (1.54) | − | 1.547 |
| P−B1 | 1.91 (1.89) | 1.91 (1.88) | 1.91 (1.88) | 1.91 (1.88) | 1.890 | 1.898[b] |
| P−B2 | − | 1.90 (1.90) | 1.91 (1.91) | 1.91 (1.90) | − | 1.897[b] |
| $\delta$ | 180.0 (180[c]) | 176.5 (180[c]) | 176.2 (180[c]) | 177.0 (180[c]) | 180.0 | 174.6 |

[a] Values in parentheses correspond to the H-subtituted models. Atomic labeling is indicated in Figure 2. [b] Average distance to the two P bonded atoms. [c] Constraint.

## Results and Discussion

In this section the most relevant aspects related to geometries, energies, the "communication" and magnetic coupling between PBPB moieties, and the low-lying states of the planar molecules, will be discussed.

**Molecular Geometries.** First of all, we perform a structural analysis of the **1**, **2**, and **3** compounds for the different conformations and substitutions. The most relevant computationally optimized and experimental bond distances and the BPPB dihedral angle are shown in Tables 1−3.

The structural parameters of the optimized PBPB unit in the planar conformation, **1A**, are in very good agreement with X-ray experimental data in the solid state[36,37] (Table 1). The optimized geometry of **1A** is also very close to previous calculations by Scheschkewitz et al.[36] at a similar level of theory. The main difference lies in the interflap angle between the two PBPB units. Whereas an angle of 180° was found in this study, Scheschkewitz's result indicates 174°. Comparison between **1A** and the H-substituted (**1AH**) system reveals one important difference. Replacing the $^i$Pr and $^t$Bu groups by hydrogen atoms at P and B, respectively, transforms the planar structure from the minimum of the potential energy surface into a first order saddle point, which has been already observed.[36] The associated imaginary frequency corresponds to the B−B bond formation process. Additionally, only slight differences between optimized

(47) Hariharan, P. C.; Pople, J. A. *Theor. Chim. Acta* **1973**, *28*, 213–222.
(48) Krishnan, R.; Binkley, J. S.; Seeger, R.; Pople, J. A. *J. Chem. Phys.* **1980**, *72*, 650–654.
(49) Frisch, M. J.; Pople, J. A.; Binkley, J. S. *J. Chem. Phys.* **1984**, *80*, 3265–3269.
(50) Vahtras, O.; Almlöf, J.; Feyereisen, M. W. *Chem. Phys. Lett.* **1993**, *213*, 514–518.
(51) Komornicki, A.; Fitzgerald, G. *J. Chem. Phys.* **1993**, *98*, 1398–1421.
(52) Feyereisen, M.; Fitzgerald, G.; Komornicki, A. *Chem. Phys. Lett.* **1993**, *208*, 359–363.
(53) Bernholdt, D. E.; Harrison, R. J. *Chem. Phys. Lett.* **1996**, *250*, 477–484.
(54) Hättig, C.; Weigend, F. *J. Chem. Phys.* **2000**, *113*, 5154–5161.
(55) Hättig, C.; Hald, K. *Phys. Chem. Chem. Phys.* **2002**, *4*, 2111–2118.
(56) Cullen, J. *Chem. Phys.* **1996**, *202*, 217–229.
(57) Voorhis, T. V.; Head-Gordon, M. *J. Chem. Phys.* **2000**, *112*, 5633–5638.
(58) Weigend, F.; Häser, M.; Patzelt, H.; Ahlrichs, R. *Chem. Phys. Lett.* **1998**, *294*, 143–152.
(59) Roos, B. O. *Int. J. Quantum Chem. Symp.* **1980**, *14*, 175–189.
(60) Casanova, D.; Head-Gordon, M. *Phys. Chem. Chem. Phys.* **2009**, *11*, 9779–9790.
(61) Parkhill, J. A.; Lawler, K.; Head-Gordon, M. *J. Chem. Phys.* **2009**, *130*, 084101.
(62) Shao, Y.; et al. *Phys. Chem. Chem. Phys.* **2006**, *8*, 3172–3191.
(63) Schmidt, M. W.; Baldridge, K. K.; Boatz, J. A.; Elbert, S. T.; Gordon, M. S.; Jensen, J. H.; Koseki, S.; Matsunaga, N.; Nguyen, K. A.; Su, S.; Windus, T. L.; Dupuis, M.; Montgomery, J. A., Jr. *J. Comput. Chem.* **1993**, *14*, 1347–1363.

***Table 2.*** Experimental and B3LYP/6-31G(d) Optimized Most Relevant Atomic Distances (in Å) and the BPPB Dihedral Angle ($\delta$ in deg) of Bicycle Singlet Structures (**B**)[a]

| | | | | | experimental |
|---|---|---|---|---|---|
| bicycle structures | **1B** | **2B** | *p*-**3B** | *m*-**3B** | *m*-**3B**[44] |
| B1−B2 | 2.44 | 1.85 | 1.85 | 1.87 | 1.892 |
| | (1.81) | (1.80) | (1.80) | (1.80) | |
| P···P | 2.79 | 2.90 | 2.90 | 2.90 | 2.861 |
| | (2.83) | (2.83) | (2.83) | (2.82) | |
| B1−$C_{tBu}$ | 1.62 | 1.62 | 1.62 | 1.63 | 1.610 |
| B2−$C_{Ph}$ | − | 1.58 | 1.58 | 1.58 | 1.575 |
| | | (1.58) | (1.56) | (1.57) | |
| P−B1 | 1.90 | 1.89 | 1.93 | 1.92 | 1.901 |
| | (1.90) | (1.90) | (1.90) | (1.90) | |
| P−B2 | − | 1.89 | 1.90 | 1.90 | 1.876 |
| | | (1.91) | (1.92[b]) | (1.91) | |
| $\delta$ | 141 | 96 | 95 | 97 | 100.2 |
| | (92) | (89) | (90) | (90) | |

[a] Values in parentheses correspond to the H-subtituted models. Atomic labeling is indicated in Figure 2. [b] Average distance to the two P bonded atoms.

and experimental **1A** and the H-substituted planar PBPB core geometries were obtained. Differences in the atomic distances are never larger than 0.03 Å (B···B in **1A**/**1AH**).

The H-substituted monomeric bicyclic compound, **1BH**, features a substantially shortened B−B bond length compared to the substituted analogue, **1B** (Table 2). This contraction is a result of the lack of steric hindrance in **1BH**, which allows the two boron atoms to approach more closely. This is accompanied by a much smaller BPPB dihedral angle in **1BH** ($\delta = 92°$) than in the fully substituted analogue ($\delta = 141°$).

Optimized structural parameters of *p*-**3A** (and *p*-**3AH**) are very close to experimental data.[44] Analogously to **1AH**, the planar *p*-**3AH** and *m*-**3AH** molecules are now second order saddle points, with two imaginary frequencies corresponding to the formation of the two B−B bonds. The main bond distance difference between *p*-**3A** and *m*-**3A** corresponds to B−$C_{Ph}$, which is less than 0.015 Å larger in the *meta* substitution. Again, there is good agreement between computed and experimental *m*-**3B** geometries. The most significant difference between *p*-**3B** and *m*-**3B** is the B−B bond distance, being ∼0.02 Å larger in the *meta* isomer. The *p*-**3BH** and *m*-**3BH** modeled structures present shorter B−B bond distances by 0.05 and 0.07 Å, respectively, than the fully substituted molecules. Dihedral angles ($\delta$ in Tables 1 and 2) are considerably smaller in the model systems. Optimized **2A** and **2B** (and their hydrogen analogues) do not present any significant particularity with respect to the **3A** and **3B** geometries. The bicyclic conformation is the most stable geometry predicted for the benzene substituted compound (**2B**), in agreement with experimental findings.[46]

Geometry optimizations for the lowest triplet state of the H-substituted **1** and **2** and the lowest triplet and quintet states for the two isomers of **3** have also been explored (Table 3). The PBPB skeleton in the triplet state of **1** and **2** adopts a planar geometry. Similarly, the geometrical preference of the two isomers of **3** in the triplet state corresponds to the linkage of a planar (**A**) and a bicylcic (**B**) unit, where the two extra α electrons are localized in the planar PBPB moiety. Planar structures, *p*-**3AH** and *m*-**3AH**, are strongly preferred for the quintet state. It is worth noting that triplet and quintet geometries relative to singlet state optimized structures present planar PBPB skeletons with much longer B−B and shorter P−P distances.

***Table 3.*** B3LYP/6-31G(d) Optimized Most Relevant Atomic Distances (in Å) and the BPPB Dihedral Angle ($\delta$ in deg) of H-Substituted Triplet and Quintet Structures[a]

| | triplets | | | | quintets | |
|---|---|---|---|---|---|---|
| | **1AH** | **2AH** | *p*-**3H** | *m*-**3H** | *p*-**3AH** | *m*-**3AH** |
| B1···B2 | 2.75 | 2.75 | 2.75 | 2.75 | 2.75 | 2.75 |
| | | | (1.85) | (1.83) | | |
| P−P | 2.70 | 2.71 | 2.71 | 2.71 | 2.71 | 2.71 |
| | | | (2.83) | (2.83) | | |
| B2−$C_{Ph}$ | − | 1.52 | 1.51 | 1.52 | 1.53 | 1.51 |
| | | | (1.56) | (1.56) | | |
| P−B1 | 1.93 | 1.92 | 1.92 | 1.92 | 1.92 | 1.93 |
| | | | (1.89) | (1.89) | | |
| P−B2 | 1.93 | 1.92 | 1.94 | 1.94 | 1.93 | 1.94 |
| | | | (1.91) | (1.91) | | |
| $\delta$ | 180 | 180 | 179 | 179 | 180 | 179 |
| | | | (94) | (92) | | |

[a] Values in parentheses for the *p*-**3H** and and *m*-**3H** triplet structures correspond to the non-planar PBPB unit (**B**). Atomic labeling is indicated in Figure 2.

***Table 4.*** B3LYP and PP Single-Point Energies (in kcal/mol) of Full and H-Substituted **3** Isomers Relative to *p*-**3A** and *p*-**3AH**, Respectively[a]

| | *p*-**3AH** | *m*-**3AH** | *p*-**3BH** | *m*-**3BH** |
|---|---|---|---|---|
| B3LYP | 0.0 | 1.8 | −16.8 | −16.3 |
| PP[b] | 0.0 | −2.3 | −17.2 | −17.2 |

| | *p*-**3A** | *m*-**3A** | *p*-**3B** | *m*-**3B** |
|---|---|---|---|---|
| B3LYP | 0.0 | 3.5 | −4.3 | −3.1 |
| PP[b] | 0.0 | 3.3 | −0.1 | 1.0 |

[a] All energies have been computed with the 6-31G(d) basis set. [b] Five pairs.

This behavior lies in the antibonding character of the through space $\pi$ interaction between boron atoms in the triplet and the quintet.

**Relative Stability.** The relative energies between the different isomers have been analyzed by B3LYP and the PP method with five active pairs. Single point energies of H-substituted models and the fully substituted molecules are shown in Table 4.

The energy gaps obtained for the H-substituted molecules are in agreement with previous calculations at the B3LYP/6-31G(d) computational level.[44] The planar isomers are 17−18 kcal/mol destabilized with respect to the **B** forms for both *para* and *meta* substitutions. Similar destabilization was already observed in the PBPB monomer calculations.[36,39,45] Energy differences between *para* and *meta* substitutions are rather small. In general, PP results are comparable to those by B3LYP. The main quantitative discrepancy is obtained in the *p*-**3AH**/*m*-**3AH** relative energies. B3LYP energies indicate the 1.8 kcal/mol larger stability of *p*-**3AH**, while in PP *m*-**3AH** is preferred by 2.3 kcal/mol.

The energy difference between the planar and bis(bicyclic) forms is drastically reduced when introducing the $^{i}$Pr and $^{t}$Bu groups. The B3LYP energy gap of *p*-**3B** to *p*-**3A** is 4.3 kcal/mol. Despite the fact that the gap is considerably smaller than in the H-substituted case, it is not in quantitative agreement with experimental observations.[44] On the other hand, the energy difference computed by restricted PP only is 0.1 kcal/mol, much more in accordance with the experimental equilibrium observed in solution between the two forms.[44]

Frequency analysis of fully and H-substituted molecules indicates that, whereas the planar model systems are second

***Table 5.*** Planar to Bicyclic SCF Energy and Thermodynamic Potential of **1** and **3** Compounds and Their H-Substituted Analogues[a]

| | ΔSCF | Δ*H* | Δ*S* | Δ*G* |
|---|---|---|---|---|
| **1AH** → **1BH** | −15.15 | −14.46 | 5.47 | −16.09 |
| *p*-**3AH** → *p*-**3BH** | −16.84 | −15.05 | 10.09 | −18.06 |
| *m*-**3AH** → *m*-**3BH** | −18.11 | −17.36 | 9.69 | −20.25 |
| **1A** → **1B** | 5.39 | 5.31 | 2.03 | 4.70 |
| *p*-**3A** → *p*-**3B** | −4.26 | −3.31 | −1.61 | −2.83 |
| *m*-**3A** → *m*-**3B** | −6.64 | −6.56 | 4.79 | −7.99 |

[a] All values were computed at the B3LYP/6-31G* level. Energies are given in kcal mol$^{-1}$, and entropy values in cal mol$^{-1}$ K$^{-1}$. Δ*G* has been computed at 298 K.

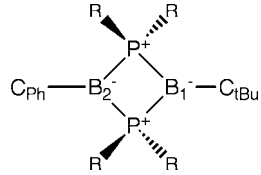


***Figure 2.*** Atomic labeling of PBPB used in the description of geometrical parameters (Tables 1−2). Although the B−B bond is not represented, labels are applicable for both planar (**A**) and bicyclic (**B**) molecules.

order saddle points on the potential energy surface, the fully substituted analogues are confirmed minima. The strong importance that the phosphorus and boron substituents have on the relative stability of the planar vs bicyclic geometries was recently discussed by Soleilhavoup et al. for the PBPB unit.[45] In their study, the authors conclude that the order of stability between planar and bicyclic forms of $^{i}$Pr and Ph substituted bond-stretch isomers is strongly entropy driven, in which the σ-bond formation is entropically favored. Equally, the entropy increases in the B−B σ-bond formation of fully and H-substituted **1** and **3** molecules studied here (Table 5). Only in the *para* substitution of **3** there is a slight entropic preference for the planar form.

In the H-substituted models the enthalpy contribution to the free energy favors the closed bicyclic forms and is responsible for a large preference over the planar conformers at standard temperature. These free energy differences are considerably reduced in the fully substituted molecules. The **1A** to **1B** reaction is clearly endothermic ($\Delta G = 4.70$ kcal/mol).

**Communication between Diradical Sites.** In order to understand to what extent the π delocalization preferentially stabilizes the *para* planar isomer, we compare the energetic cost of twisting 90° the phenyl ring with (a) and without (b) the second PBPB unit in *para* isomers (Figure 3). We define the energy difference between the two cases as *delocalization energy* ($E_D = E^{(a)}_{twist} - 2E^{(b)}_{twist}$), which should give us an estimate of the communication between the two diradical sites through the π system.

The delocalization energy obtained for *p*-**3AH** ($E_D = 1.6$ kcal/mol) coincides well with the computed energy difference to *m*-**3AH** (1.8 kcal/mol in Table 4). Thus, this indicates that, in the H-substituted case, the communication through the π framework is the main driving force of the *para* versus *meta* stabilization, as has been previously suggested.[46] The same analysis on the fully substituted system yields a very similar delocalization energy ($E_D = 1.4$ kcal/mol), but now $E_D$ only corresponds to one-third of the energy gap between *p*-**3A** and *m*-**3A** (Table 4). One possible reason for the increased gap could be the 10° and 4° deviation of coplanarity by the PBPB groups in *m*-**3A**, not present in *p*-**3A** (CCBP dihedral: ∼3°). However, setting the dihedral angles in *m*-**3AH** to −10° and −4° only yields a tiny energy increase (∼0.1 kcal/mol) which cannot account for the remaining 2.8 kcal/mol.

These results suggest that steric and/or electronic factors due to the presence of $^{i}$Pr and $^{t}$Bu groups are responsible for the remaining two-thirds of the *para* to *meta* energy gap of **3A**. Indeed, *m*-**3A** exhibits much larger steric hindrance than *p*-**3A**. Although both substitutions contain two nonbonded hydrogen distances between one of the $^{i}$Pr groups and the phenylene linker which fall within the van der Waals range (2.18−2.40 Å),[64,65] these are ∼0.1 Å shorter in the *meta* isomer, i.e. 2.17−2.21 Å and 2.28−2.29 Å in *m*-**3A** and *p*-**3A**, respectively. In addition, the $^{i}$Pr groups from different PBPB units are much closer in *m*-**3A**, with the smallest H···H separation being 2.35 Å, while in *p*-**3A** these H···H distances are never shorter than 5.5 Å. Some of the short distances in *m*-**3A** are shown in Figure 4.

**Radical Character.** In this section the radicaloid character of the singlet state under consideration will be explored. The chemical intuition of radical character is linked to the number of unpaired electrons, but it has no unique mathematical definition.[66] In terms of theoretical assessment techniques, one of the most basic and commonly applied ways to quantify the radical character is to determine natural orbital occupation numbers.[67−71] Thereby, radicals are regarded as species whose orbital occupations deviate substantially from zero or two. This approach was discussed in detail by Döhnert and Koutecký.[71]

Among the unlimited possibilities to quantify the effective number of unpaired electrons, we employ the mathematical expression proposed by Head−Gordon[69] (eq 1).

$$N_U = \sum_{i=1}^{M} (1 - \mathrm{abs}(1 - n_i)) \qquad (1)$$

where $\{n_i\}$ are the natural occupation numbers obtained from the M × M one-particle density matrix. $N_U$ values obtained by PP, CASSCF, and RAS-2F are presented in Table 6 for fully and H-substituted planar molecules.

There is almost no difference between the amounts of unpaired electrons obtained for *para* and *meta* molecules. The chemical substitution in boron and phosphorus atoms, i.e. H-substitution or alkyl groups, does not significantly alter the computed values. PP with two active pairs indicates 0.75−0.77 unpaired electron. These numbers become larger (∼0.15 electron) when the six π electrons of the benzene ring are also considered in the active space (PP with five pairs). CASSCF(4,4) and RAS-2SF results are very close to PP with two and five correlated pairs, respectively. The moderate extent of radical character obtained (the theoretical $N_U$ limit corresponds to four unpaired electrons) is probably the reason for the large stability of such species.

Although $N_U$ of *para* and *meta* molecules indicate almost identical numbers of unpaired electrons, an inspection of the electronic occupations of RAS-2SF and CASSCF(4,4) frontier

(64) Rowland, R. S.; Taylor, R. *J. Phys. Chem.* **1996**, *100*, 7384–7391.
(65) Bondi, A. *J. Phys. Chem.* **1964**, *68*, 441–451.
(66) Dutoi, A. D.; Jung, Y.; Head-Gordon, M. *J. Phys. Chem. A* **2004**, *108*, 10270–10279.
(67) Bonačić-Koutecký, V.; Koutecký, J.; Michl, J. *Angew. Chem., Int. Ed. Engl.* **1987**, *26*, 170–189.
(68) Staroverov, V. N.; Davidson, E. R. *J. Am. Chem. Soc.* **2000**, *122*, 186–187.
(69) Head-Gordon, M. *Chem. Phys. Lett.* **2003**, *372*, 508–511.
(70) Flynn, C. R.; Michl, J. *J. Am. Chem. Soc.* **1974**, *96*, 3280–3288.
(71) Döehnert, D.; Koutecký, J. *J. Am. Chem. Soc.* **1980**, *102*, 1789–1796.

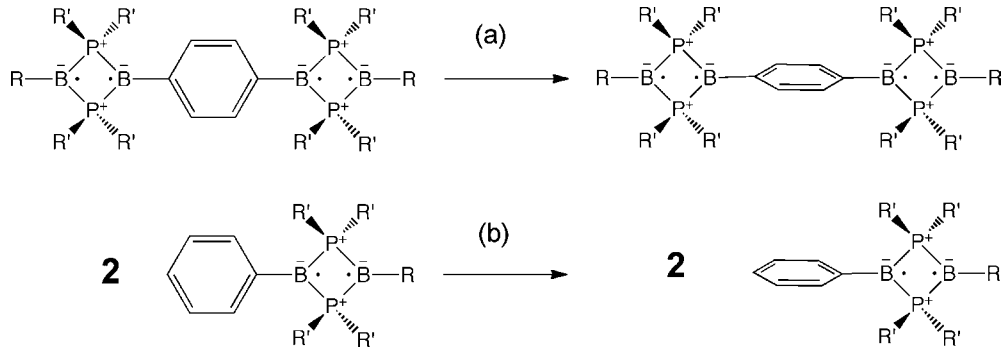


***Figure 3.*** Delocalization energy in *para* isomers. Delocalization energy is defined as the difference between the energy cost of twisting the phenyl ring (a) and two times the twisting energy without one of the PBPB units (b). The same scheme is applied for fully (*p*-**1A**, $R = {}^{i}$Pr, $R' = {}^{t}$Bu) and H-substituted (*p*-**1AH**, R, $R' =$ H) molecules.

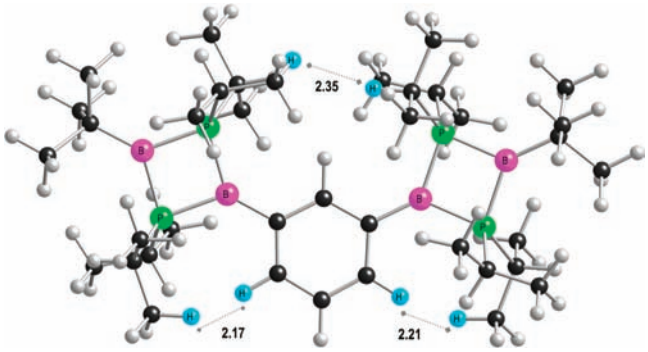


***Figure 4.*** B3LYP/6-31G(d) optimized geometry of *m*-**3A** with some short H···H distances indicated (in Å).

***Table 6.*** Computed Effective Unpaired Electrons $N_U$ (eq 1) of Planar Dimer Molecules

| | *p*-3AH | *m*-3AH | *p*-3A | *m*-3A |
|---|---|---|---|---|
| PP[a] | 0.77 | 0.77 | 0.75 | 0.76 |
| PP[b] | 0.90 | 0.92 | 0.87 | 0.91 |
| CASSCF | 0.79 | 0.77 | 0.77 | 0.76 |
| RAS-2SF | 0.89 | 0.88 | 0.88 | 0.88 |

[a] Two pairs. [b] Five pairs.

orbitals shows different behavior in the electron distribution of the two isomers (Figure 5). While the electron occupation in the LUMO+1 is 20% lower than in the LUMO in *p*-**3AH**, the ~0.4 electron is distributed evenly between the two lowest unoccupied orbitals in *m*-**3AH**. In other words, the *para* substitution shows a clear preference for the $\pi$-bonding interaction between the two molecular ends, while $\pi$-bonding/$\pi$-antibonding interactions through the phenylene linker are hardly distinguished in *m*-**3AH**. A similar analysis can be carried out from the HOMO and HOMO−1 occupations.

At this point, we have analyzed the radical character by means of the effective unpaired electrons (eq 1), but we still must face the question to what extent the singlet ground state of *p*-**3A** and *m*-**3A** should be considered tetraradicaloids. One possibility for quantifying this property is by extending the electronic structure properties of a singlet diradicaloid to a tetraradicaloid species, e.g. the extent of open shell singlet character. For a system featuring four unpaired electrons, an open shell singlet can be achieved by coupling two singlet or two triplet units, respectively. The former can be interpreted as communication between two singlet diradical sites. The latter constitutes a novel configuration, which corresponds to the concomitant excitation of the two subunits and could be used to discern between two interacting diradical moieties (two sets of two strongly correlated electrons) and a true tetraradical (four strongly correlated electrons).

Therefore, analogous to the utilization of the $t_2$ magnitude at times as an indicator of the extent of diradical character,[72] we will focus our attention to the weight of the simultaneous excitation of four electrons, defined by the $t_4$ coupled cluster amplitude, as a measure of the tetraradical character. Since PP calculations only include double excitations, any cooperative behavior between the two groups will not be reflected by this method. For this reason we analyze the magnitude of the $t_4$ amplitude from the doubly occupied HOMO−1 and HOMO to the LUMO and LUMO+1 orbitals (Figure 6) computed by the perfect quadruples (PQ) extension of PP. On the other hand, CASSCF(4,4) and RAS-2SF incorporate up to quadruple excitations in the active configuration interaction (CI) space. The concomitant $t_4$ cluster amplitude can be approximated by decomposition of the computed $\{c_i, i = 1,2,3,4\}$ amplitudes and through the relations between CI and CC excitation operators at the FCI limit. These results are summarized in Table 7, where intermediate normalization has been applied.

The $t_4$ values recovered indicate a small interaction between the two PBPB units. These results become even clearer when comparing the weight due to the simultaneous interaction of four electrons to the entire set of possible mechanisms involving four electrons contained in CASSCF and RAS-2SF. The RAS-2SF $t_4$ amplitude represents only 3.3% of $c_4$ in *p*-**3AH** and 2% in *m*-**3AH**, while it is less than 1% in CASSCF for both isomers. It is also worth mentioning that all methods predict larger coupling in the *para* isomer. Considering the almost identical values of unpaired electrons between fully and H-substituted molecules obtained in the previous section (Table 6), we expect the $t_4$ values to be fully transferable to the $^{i}$Pr and $^{t}$Bu substituted molecules.

**Low-Lying Excited States and Magnetic Couplings.** Spin-state energy gaps are commonly used to characterize radicals. In particular singlet−triplet splitting is one of the most widely used indicator of diradical character.[73] The same idea is used here for the studied tetraradical systems. In this sense, in addition to the singlet ground state, we use RAS-2SF to compute the low-lying excited singlet, three triplets, and the quintet state of *p*-**3A** (*p*-**3AH**) and *m*-**3A** (*m*-**3AH**) molecules (Table 8 and Figure 7).

There are only small differences between the excitation energies of full and H-substituted molecules. When alkyl groups are taken into account the excitation energies are slightly reduced

(72) Li, X.; Paldus, J. *J. Chem. Phys.* **2008**, *129*, 174101.
(73) Davidson, E. R. In *Diradicals*; Borden, W. T., Ed.; Wiley-Interscience: New York, 1982.

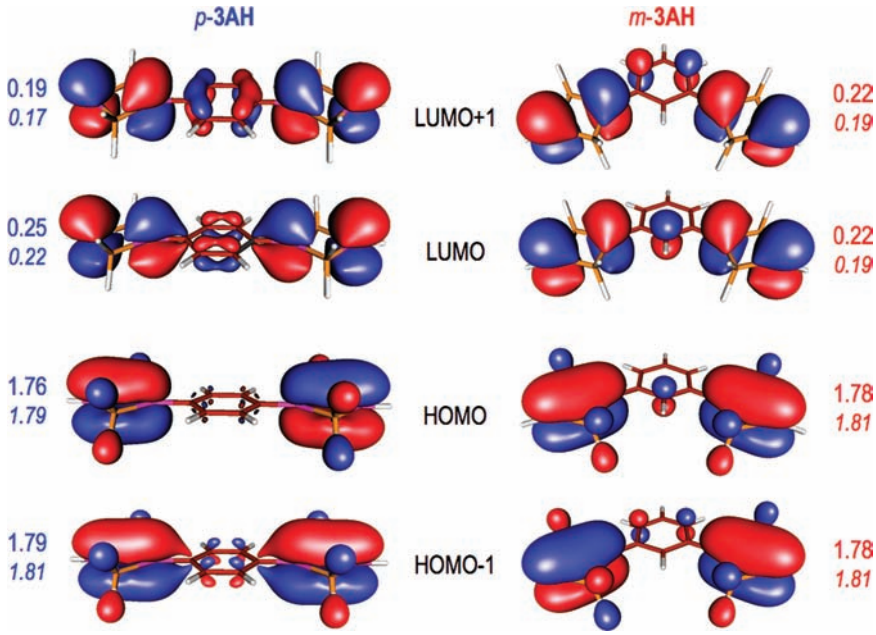


***Figure 5.*** RAS-2SF natural orbitals of *p*-**3AH** and *m*-**3AH**. RAS-2SF and CASSCF(4,4) (in italics) orbital occupations are also indicated.

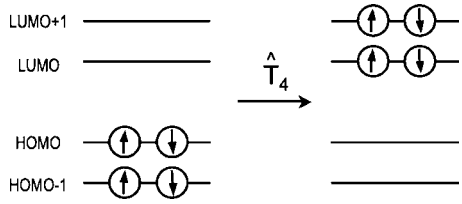


***Figure 6.*** Diagrammatic representation of the quadruple cluster excitation from the HOMO−1 and HOMO to the LUMO and LUMO+1 orbitals.

***Table 7.*** Cluster Quadruple Amplitude Excitations ($t_4$) from PQ, CASSCF(4,4), and RAS-2SF Computations of *p*-**3AH** and *m*-**3AH**[b]

| | *p*-3AH | *m*-3AH |
|---|---|---|
| CASSCF | 0.0009 | 0.0005 |
| RAS-2SF | 0.0037 | 0.0023 |
| PQ[b] | 0.0178 | 0.0110 |

[a] Intermediate normalization of the wave function has been considered. [b] Optimized orbitals from PP with two active pairs.

***Table 8.*** Vertical Excitation Energies (in kcal/mol) of *p*-**3AH**/*p*-**3A** and *m*-**3AH**/*m*-**3A** Low-Lying Singlet, Triplet, and Quintet States Computed by RAS-2SF/6-31G(d)

| | sym | *p*-3AH | *p*-3A | sym | *m*-3AH | *m*-3A |
|---|---|---|---|---|---|---|
| $S_1$ | $^1A_{1g}$ | 42.4 | 41.1 | $^1A_1$ | 49.1 | 47.9 |
| $T_1$ | $^3B_{3u}$ | 21.0 | 20.5 | $^3A_1$ | 23.4 | 23.0 |
| $T_2$ | $^3A_{1g}$ | 25.1 | 24.7 | $^3B_1$ | 24.1 | 23.6 |
| $T_3$ | $^3B_{3u}$ | 45.7 | 44.6 | $^3B_1$ | 48.6 | 47.5 |
| $Q_1$ | $^5A_{1g}$ | 50.5 | 49.4 | $^5A_1$ | 47.6 | 46.5 |

by 0.4−1.2 kcal/mol. The two lowest triplets, e.g. $T_1$ and $T_2$, lie 20−25 kcal/mol above the singlet ground state in both isomers, but in *p*-**3A** (*p*-**3AH**) the energy separation between $^3B_{3u}$ and $^3A_{1\,g}$ is close to 4 kcal/mol, while in *m*-**3A** (*m*-**3AH**) the two triplets, $^3A_1$ and $^3B_1$, are only 0.6 kcal/mol apart. The *para* and *meta* highest triplets correspond to doubly excited configurations with $B_{3u}$ and $B_1$ symmetries, respectively. The first excited singlet state ($S_1$) is mainly built up from similar contributions of doubly excited closed shell configurations from the closed shell single determinant (Hartree−Fock like) ground

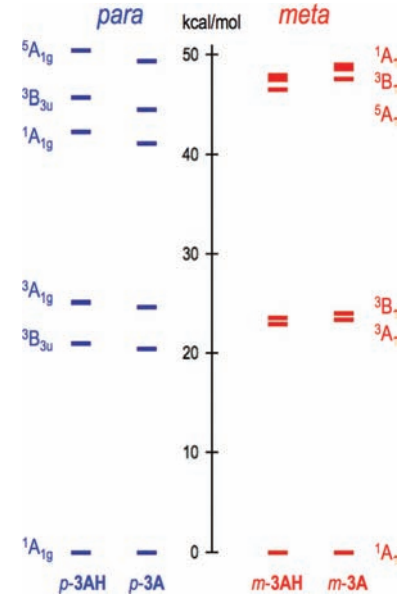


***Figure 7.*** State energy diagram (in kcal/mol) computed at the RAS-2SF/6-31G(d) computational level for *p*-**3A**, *p*-**3AH**, *m*-**3A**, and *m*-**3AH**. All energies are given with the respective ground state as reference.

state. Finally, the $M_S = 0$ quintet state is obtained as the totally symmetric combination of four unpaired electrons in the four frontier orbitals (Figure 5).

Despite the lack of dynamical correlation in RAS-2SF, it is been shown[60] that the balanced treatment of low-lying states of radicaloid systems makes it very suitable in the computation of energy gaps. At the same time, the reader should be rather cautious in taking the results presented above as a benchmark for the vertical transitions of *p*-**3A** and *m*-**3A**.

**Magnetic Couplings.** Some of the features of *para* and *meta* PBPB dimers computed vertical excitation energies can be rationalized through the phenomenological Heisenberg Hamiltonian (eq 2) that describes the exchange interaction between paramagnetic centers.

$$\hat{H} = -\sum_{i<j} J_{ij}\hat{S}_i\hat{S}_j \qquad (2)$$

where $\hat{S}_i$ and $\hat{S}_j$ are the total spins in each paramagnetic center, and $J$ is known as the exchange constant.[74] Positive $J$ values indicate ferromagnetic interaction (parallel spins), while negative values correspond to antiferromagnetic coupling (antiparallel spins). The application of the Heisenberg model to *p*-**3A** (*p*-**3AH**) and *m*-**3A** (*m*-**3AH**) can be used to describe the interaction between the four boron atoms ($S = 1/2$). As a simple approximation of the four-center problem, we only take two kinds of magnetic couplings into account: the short-range interactions ($\sigma$) between the two boron atoms in the same PBPB skeleton and a long-range interaction ($\lambda$) through the phenylene linker (centers 2 and 3 in Figure 8), i.e. only interactions between nearest neighbors.

The short-range interaction coincides with the singlet−triplet energy gap of the PBPB core. On the other hand, the magnitude of $\lambda$ is a direct measure of the communication between PBPB cores. Considering two noninteracting PBPB units as the zero order approach and for antiferromagnetic $\sigma$ interactions ($\sigma < 0$), the most stable state has singlet spin multiplicity, with two triplet states at $\sigma$ and three higher states (singlet, triplet and quintet) at $2\sigma$ energy separations (Figure 9, $\lambda = 0$). When the $\lambda$ interaction is switched on, the degenerate states split in accordance with the magnitude and sign of $\lambda$. The larger the communication between diradical sites, the larger the separation between states. The nature of the $\lambda$ interaction, ferro- or antiferromagnetic, is responsible for the stabilization or destabilization of the different states (Figure 9).

The $\sigma$ and $\lambda$ values of the nearest neighbors Heisenberg model for *p*-**3A**, *m*-**3A**, and the H-substituted analogues are shown in Table 9.[75] The short-range coupling ($\sigma$) is by far the strongest interaction, being more than 3 times larger than $\lambda$ in *p*-**3A** (*p*-**3AH**) and almost 20 times larger in *m*-**3A** (*m*-**3AH**). In both isomers, $\sigma$ is responsible for having a singlet ground state, indicating the interaction of two singlet subunits, rather than two triplet moieties. This is in accordance with the small $t_4$ amplitudes obtained for the two species (Table 7). As expected by the polarization rule, $\lambda$ indicates antiferro- and ferromagnetic couplings for the *para*-phenylene and *meta*-phenylene linkers, respectively. The magnitude of long-range interaction is more than 2 times larger in the *para* isomer.

Comparison of the nearest neighbors approach of the Heisenberg model with the energy diagrams of the two isomers (Figure 7) indicates relevant differences between *para* and *meta* substitutions. The appreciable energy gap between $^3B_{3u}$ and $^3A_{1g}$ (and $^1A_{1g}$, $^3B_{3u}$, and $^5A_{1g}$) in *p*-**3A** is further proof of the communication through the *para*-phenylene linker. The near degeneracy of *m*-**3A** states indicates a very weak interaction. In addition, the state energy ordering in *p*-**3A** corresponds to an antiferromagnetic interaction, while in *m*-**3A** the parallel alignment is preferred.

## Conclusions

The main geometrical characteristics of the PBPB monomer (**1**), phenyl substituted PBPB (**2**), and PBPB dimer (**3**) have been described and compared to experimental data. The importance of $^i$Pr and $^t$Bu groups in the stability of the planar isomers is clearly manifested in the relative energies and frequency calculations reported. The H-substituted models show a clear preference for the bicyclic form in both isomers. When the full substitution is considered, there is a systematic stabilization of the planar forms compared to the H-models. Frequency analysis has been discussed at the B3LYP/6-31G(d) computational level. Thermodynamic potentials for the planar to bicyclic bond formation reactions have been presented and compared to experimental stabilities.

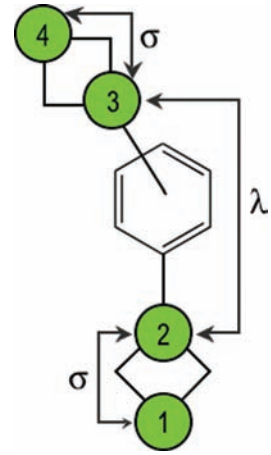


***Figure 8.*** Four paramagnetic center model for the *para* and *meta* systems. First neighbors exchange constants ($\sigma$ and $\lambda$) are indicated by arrows between centers.

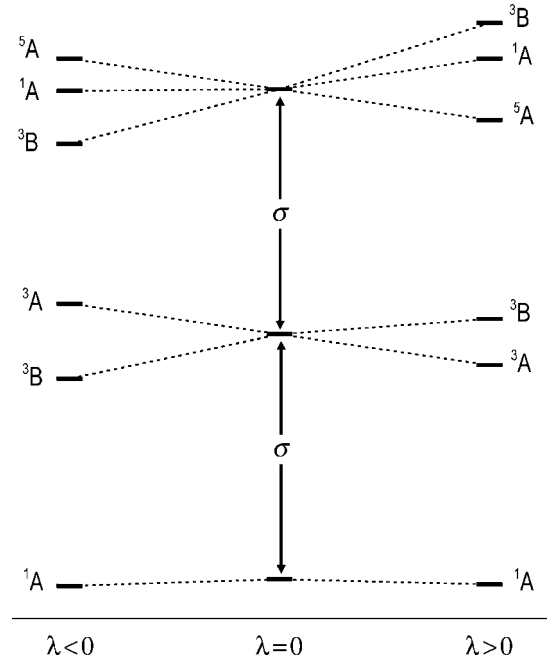


***Figure 9.*** Short ($\sigma$) and long ($\lambda$) range energy splitting in the four paramagnetic center models of Figure 8. A and B indicate symmetrical and asymmetrical rotation around the principal axis, respectively.

***Table 9.*** Magnetic Coupling Constants (in kcal/mol) Computed by RAS-2SF/6-31G(d) of the *p*-**3A** (*p*-**3AH**) and *m*-**3A** (*m*-**3AH**) Molecules

| | *p*-**3A** | *m*-**3A** |
|---|---|---|
| $\sigma$ | −22.6 (−23.1) | −23.3 (−23.7) |
| $\lambda$ | −7.4 (−7.1) | 1.2 (1.3) |

(74) Van Vleck, J. H. *The Theory of Electric and Magnetic Susceptibilities*; Oxford University Press: Oxford, 1932.
(75) The three lowest states ($S_0$, $T_1$, and $T_2$) have been considered in the computation of short and long range magnetic couplings.

Electronic structure calculations have confirmed the ground state singlet spin multiplicity ($S = 0$). The overall radical character of the planar molecules has been computed and rationalized by PP, PQ, CASSCF, and RAS-2SF methods. The lowest excited singlet, triplet, and quintet states have been calculated by RAS-2SF.

The extent of the so-called "communication" between PBPB moieties has been analyzed by means of the delocalization energy ($E_D$), the effective number of unpaired electrons, the energy gaps between excited states, and the resolution of the nearest neighbors Heisenberg model. All explored approaches indicate the presence of a weak interaction between two singlet PBPB units, with the *para* isomer featuring more "communication" than the *meta* substituted system. From the results obtained in this study, it is rather questionable that the catenation of singlet PBPB moieties via *para*-phenylene linkage could yield metallic polymers. This situation is the result of the substantial difference between short- and long-range couplings ($\sigma$ and $\lambda$, respectively). To overcome this problem, one possibility is to search for other antiferromagnetic linkers which yield larger $\lambda$ values. However, *para*-phenylene is known to be one of the strongest antiferromagnetic linkers. Therefore, the most likely solution would be to weaken the coupling within the PBPB moiety, maybe through appropriate substitution at the B and P centers.

**Acknowledgment.** Financial support for this work was provided by the Office of Basic Energy Sciences of the U.S. Department of Energy through the LBL Ultrafast Center, with additional support from the Director Office of Energy Research, Office of Basic Energy Sciences, Chemical Sciences Division of the U.S. Department of Energy under Contract DE-AC0376SF00098, and supercomputer time from NERSC. F.B. thanks doctor Keith Lawler for his comments and suggestions on several of the topics presented in this work. D.C. gratefully acknowledges the Ramón y Cajal program for financial support.

**Supporting Information Available:** Complete ref 62. The absolute energies and optimized geometries of fully and H-substituted molecules in the lowest singlet state. This material is available free of charge via the Internet at http://pubs.acs.org.

JA104772W